

Thermally relativistic flows induced by gravitational-force-free particle motion in curved spacetime

Ryosuke Yano^{*}

Department of Advanced Energy, University of Tokyo, 5-1-5 Kashiwanoha, Kashiwa, Chiba 277-8561, Japan

Kojiro Suzuki[†]

Department of Advanced Energy, University of Tokyo, 5-1-5 Kashiwanoha, Kashiwa, Chiba 277-8561, Japan

Hisayasu Kuroda[‡]

Department of Information Technology, University of Ehime, 3 Bunkyo-cho, Matsuyama, Ehime 790-8577, Japan

(Received 10 May 2009; published 4 December 2009)

Thermally relativistic flows in the early Universe can be characterized by the emergence of flows induced by gravitational-force-free particle motion in curved spacetime as well as induced by the gravitational force. In this paper, thermally relativistic flows induced by gravitational-force-free particle motion in curved spacetime are discussed on the basis of the general relativistic Boltzmann equation. As an object of analysis, we consider the flow from the static state inside the Schwarzschild radius of a thermally relativistic stuffed black hole induced by such motion. Analytical results obtained using the collisionless, nongravitational general relativistic Boltzmann equation reveal that the initial cluster is induced by gravitational-force-free particle motion. Numerical results obtained using the nongravitational general relativistic Anderson-Witting model confirm the presence of an initial cluster inside the thermally relativistic stuffed black hole, which is induced by gravitational-force-free particle motion.

DOI: [10.1103/PhysRevD.80.123506](https://doi.org/10.1103/PhysRevD.80.123506)

PACS numbers: 98.80.Jk

I. INTRODUCTION

In the early Universe, space was filled with high-energy, high-density fluctuating matter [1]. In such a fluctuating field [2], strongly curved spacetime can be formed as a result of a local solution of Einstein's equation [3]. Consequently, primordial black holes are often considered [4] to have existed in the early Universe. In discussions on the dynamics of matter in strongly curved spacetime, the flow of matter is considered to be induced exclusively by the gravitational force, which is represented by the equation of the particle motion via Christoffel symbols [3]. However, when the curved spacetime is filled with thermally relativistic matter, this flow of matter can be induced not only by the gravitational force but also by the free motion of the particle, because the local equilibrium distribution function depends on the local metric of the curved spacetime [5]. On the basis of the relativistic kinetic theory, the flow of matter is considered to be induced by the local gradient of the distribution function due to the local gradient of the metric of the spacetime as well as induced by the gravitational force. When the thermal energy of matter increases, this dependency of the equilibrium distribution function on the metric of the spacetime becomes stronger. Consequently, when the thermal energy of the matter in curved spacetime increases, the flow induced by such

gravitational-force-free particle motion becomes less negligible compared with the flow induced by the gravitational force. As an initial attempt to clarify such thermally relativistic flows in the early Universe, we analyzed the flow induced by the gravitational-force-free particle motion in curved spacetime by using the general relativistic kinetic theory.

In this paper, we assumed an isotropic field filled with matter whose thermal energy is relativistic. To avoid the difficulties involved with the excision of the characteristic point [3] in the Schwarzschild metric, we used the Friedmann-Robertson-Walker (FRW) metric [3] as the initial gauge condition in the early Universe. As the primordial black hole generated by thermally relativistic matter in the early Universe, a stuffed black hole [6] is considered here on the basis of no-hair theorem [7] of a black hole, although the stuffing process involves a region that does not satisfy Einstein's equation [6]. To solve Einstein's equation, we used the Z4 formalism [8] by Bona *et al.*, since previous results [6,9] on the evolution of a stuffed black hole have been reported. The free parameters used in the Z4 formalism (see Appendix B) usually determine the slice condition and stability of the scheme [8]. In our numerical analysis, such free parameters must be carefully selected to avoid the numerical formation of tachyons. Throughout this numerical analysis, a hard-sphere particle [5] is assumed to be the basic component of matter. The effects due to inflation [10] and quantum mechanics [11] are not considered. In particular, the decrease in the temperature caused by Hawking's

^{*}yano@daedalus.k.u-tokyo.ac.jp

[†]kjsuzuki@k.u-tokyo.ac.jp

[‡]kuroda@mt.y.jp

radiation [12] is excluded. Under such an assumption, the thermally relativistic field holds. Analytical results obtained using the collisionless, nongravitational general relativistic Boltzmann equation suggest the incipient flow into the center of a black hole inside the Schwarzschild radius, namely, “initial cluster” induced by gravitational-force-free particle motion. In the presence of particle collisions, such an initial cluster has been numerically confirmed by solving the nongravitational general relativistic Anderson-Witting model [13].

In Sec. II of this paper, the general relativistic Boltzmann equation is rewritten for a (3 + 1) Arnowitt-Deser-Misner (ADM) system [14] by changing its momentum space into velocity space. In Sec. III A, the initial cluster induced by gravitational-force-free particle motion in curved spacetime inside the Schwarzschild radius of a thermally relativistic stuffed black hole is analytically considered on the basis of the strict solution of the collisionless, nongravitational general relativistic Boltzmann equation. In Sec. III B, the numerical results confirm the existence of such an initial cluster from the static state by solving the nongravitational general relativistic Anderson-Witting model coupled to Einstein’s equation.

II. GENERAL RELATIVISTIC BOLTZMANN EQUATION IN (3 + 1) ADM SYSTEM

The general relativistic Boltzmann equation with the distribution function based on four-momentum p^μ is written as

$$p^\mu \frac{\partial f}{\partial x^\mu} - \Gamma_{\mu\nu}^i p^\mu p^\nu \frac{\partial f}{\partial p^i} = L[f], \quad (1)$$

where f is the distribution function defined by $f \equiv f(x^\mu, p^i)$, ($i = 1, 2, 3$), $\Gamma_{\mu\nu}^i$ is the Christoffel symbol, and $L[f]$ is the collision term [13]. In numerical analysis, the treatment of momentum space is difficult, because p^μ approaches infinity as the velocity of particles approaches the speed of light. As a result, the accurate numerical integration of the distribution function in momentum space becomes difficult when the number of particles with velocity near the speed of light is non-negligible. The use of velocity space instead of momentum space as the phase space of the distribution function is therefore expected to yield a more accurate integration of the distribution function, because the velocity space is bounded by the metric [5]. For accurate integration, we must therefore derive the general relativistic Boltzmann equation on the basis of the velocity space instead of the momentum space, namely, $f(x^\mu, p^i) \rightarrow f(x^\mu, v^i)$.

The Liouville law gives the following relation for the distribution function:

$$\frac{df(x^\mu(\tau^*), v^i(\tau^*))}{d\tau^*} = \frac{\partial f}{\partial x^\mu} \frac{dx^\mu}{d\tau^*} + \frac{\partial f}{\partial v^i} \frac{dv^i}{d\tau^*}, \quad (2)$$

Here, $\tau^* = \tau/m$, where τ is the proper time and m is the

mass of a particle. To derive $dv^i/d\tau^*$, we use the equation of motion of a particle under a gravitational field

$$\begin{aligned} \frac{dp^i}{d\tau^*} &= -\Gamma_{\mu\nu}^i p^\mu p^\nu, \\ \left(\text{where } p^\mu \equiv \frac{dx^\mu}{d\tau^*}\right) &= \Gamma(v) \frac{d\Gamma(v) v^\mu}{dt} \\ &= -\Gamma_{\mu\nu}^i \Gamma(v)^2 v^\mu v^\nu, \end{aligned} \quad (3)$$

where $\Gamma(v)$ is defined as follows by using a (3 + 1) ADM system [14] with the lapse α , intrinsic curvature γ_{ij} , and zero shift $\beta^i = 0$ [14]:

$$\begin{aligned} \Gamma(v) &\equiv \frac{dt}{d\tau} = \frac{1}{\sqrt{\alpha^2 - \hat{v}^2}}, \\ \text{where } v^i &= \frac{dx^i}{dt}, \quad \hat{v}^2 \equiv \gamma_{ij} v^i v^j / c^2. \end{aligned} \quad (4)$$

From Eq. (4), $\hat{v} < \alpha$, and thus $\psi^i = dv^i/dt$ is defined as QCR

$$\begin{aligned} \psi^i &= \frac{dv^i}{dt} = \mathcal{Q} v^i - \mathcal{C}^i + \frac{v^i}{\alpha^2} \mathcal{R}_j \mathcal{C}^j, \quad \mathcal{C}^i = \Gamma_{\mu\nu}^i v^\mu v^\nu, \\ \mathcal{R}_j &= \gamma_{jk} v^k, \quad \mathcal{Q} = \mathcal{S} + \sum_{i,j=1}^3 \gamma_{ij} \mathcal{S}_{ij}, \end{aligned} \quad (5)$$

where \mathcal{S} and \mathcal{S}_{ij} in Eq. (5) are defined as

$$\mathcal{S} \equiv \partial_t \alpha \quad (6)$$

$$\mathcal{S}_{ij} \equiv \partial_t \gamma_{ij}. \quad (7)$$

Substituting Eq. (5) into Eq. (2) yields the general relativistic Boltzmann equation based on the velocity space

$$\frac{\partial f}{\partial t} + v^i \frac{\partial f}{\partial x^i} + \psi^i \frac{\partial f}{\partial v^i} = \frac{1}{\Gamma(v)} L[f]. \quad (8)$$

The first and second moments, N^μ and $T^{\mu\nu}$, are obtained by evaluating [5]

$$N^\mu = c \int_{\mathcal{R}^3} p^\mu f \sqrt{g} \frac{d^3 p}{p_0}, \quad (9)$$

$$T^{\mu\nu} = c \int_{\mathcal{R}^3} p^\mu p^\nu f \sqrt{g} \frac{d^3 p}{p_0}, \quad (10)$$

where c is the speed of light in the Minkowski metric and $g \equiv \det(g_{\mu\nu})$, in which $g_{\mu\nu}$ is the metric tensor.

Rewriting Eqs. (9) and (10) with momentum space \mathcal{R}^3 replaced by velocity space \mathcal{V}^3 yields the following:

$$N^\mu = m^3 c \int_{\mathcal{V}^3} \Gamma(v)^5 v^\mu f \sqrt{g} d^3 \mathbf{v}, \quad (11)$$

$$T^{\mu\nu} = m^4 c \int_{\mathcal{V}^3} \Gamma(v)^6 v^\mu v^\nu f \sqrt{g} d^3 \mathbf{v}. \quad (12)$$

The Eckart decomposition [15] yields the projected mo-

ments, number density n , pressure deviator $p^{(\mu\nu)}$, static pressure p , dynamic pressure ϖ , and energy per particle e as follows:

$$n = \frac{1}{c^2} N^\nu U_\nu, \quad (13)$$

$$p^{(\mu\nu)} = (\Delta_\gamma^\mu \Delta_\delta^\nu - \frac{1}{3} \Delta^{\mu\nu} \Delta_{\gamma\delta}) T^{\delta\gamma} \quad (14)$$

$$p + \varpi = -\frac{1}{3} \Delta_{\mu\nu} T^{\mu\nu}, \quad (15)$$

$$q^\mu = \Delta_\gamma^\mu U_\nu T^{\nu\gamma}, \quad (16)$$

$$e = \frac{1}{nc^2} U_\mu T^{\mu\nu} U_\nu, \quad (17)$$

where $U^\mu = \Gamma(u)u^\mu$, in which $u^\mu = (c, u^i)$, u^i is the flow velocity of the i -th component and $\Gamma(u) = 1/\sqrt{\alpha^2 - \gamma_{ij}u^i u^j/c^2}$, and where $U_\mu = \Gamma(u)u_\mu$, in which $u_\mu = (\alpha^2 c, -u^j \gamma_{ij})$ is the covariant four-velocity of the flow [15]. The projector $\Delta_{\mu\nu}$ is defined as [15]

$$\Delta_{\mu\nu} = g_{\mu\nu} - \frac{U_\mu U_\nu}{c^2}. \quad (18)$$

III. THERMALLY RELATIVISTIC FLOW INDUCED BY GRAVITATIONAL-FORCE-FREE PARTICLE MOTION IN CURVED SPACETIME

The flow in curved spacetime is induced exclusively by the gravitational force, which is revealed by the term $\psi^i \partial f / \partial v^i$ in Eq. (8), when particles are thermally nonrelativistic (i.e., $10^2 \ll \zeta = mc^2/(k\theta)$, where θ is temperature and k is Boltzmann's constant).

When particles are thermally relativistic (i.e., $1 < \zeta < 10^2$) or thermally ultrarelativistic (i.e., $(\zeta \leq 1)$), however, the flow in curved spacetime is also induced by gravitational-force-free particle motion, which is revealed by the term $v^i \partial f / \partial x^i$ in Eq. (8).

This nongravitational thermally relativistic flow is caused by the dependence of the equilibrium function, or the so-called Maxwell-Jüttner function [5], on the local lapse and intrinsic curvature. The Maxwell-Jüttner function is written as

$$f^{(0)}(x^\mu, \mathbf{v}) = \frac{n}{4\pi m^2 c k \theta K_2(\zeta)} e^{-((U^\mu p_\mu)/k\theta)}, \quad (19)$$

where p_μ is $p_\mu = m\Gamma(v)(\alpha^2 c, -v^j \gamma_{ij})$ and $K_2(\zeta)$ is the modified Bessel function of the second kind. To focus on flows induced by gravitational-force-free particle motion, we consider the following nongravitational [i.e., $\psi^i = 0$ in Eq. (8)] and collisionless [i.e., $L[f] = 0$ in Eq. (8)] general relativistic Boltzmann equation

$$\frac{\partial f}{\partial t} + v^i \frac{\partial f}{\partial x^i} = 0. \quad (20)$$

The solution of Eq. (20) is given by

$$f(t, x^i, v^i) = f(0, x^i - v^i t, v^i). \quad (21)$$

From Eq. (21), flow is not induced when $f(0, x^i - v^i t, v^i) = f(0, x^i, v^i)$. Assuming the initial conditions under which $n(0, x^i) = n_\infty$, $\zeta(0, x^i) = \zeta_\infty$, $u^i(0, x^i) = u_\infty^i$ and assuming that the distribution function follows the Maxwell-Jüttner function, the initial form of the distribution function depends on the lapse $\alpha(0, x^i)$ and the intrinsic curvature $\gamma_{ij}(0, x^i)$. As a result of these assumptions, the solution of Eq. (20) is $f(t, x^i, v^i) \neq f(0, x^i, v^i)$ when $\alpha(0, x^i)$ and $\gamma_{ij}(0, x^i)$ are not spatially uniform. The spatial difference in $f^{(0)}$ due to the spatial variability of α and γ_{ij} increases when ζ_∞ decreases. In other words, the spatial difference in $f^{(0)}$ due to curved spacetime becomes the most significant factor in the thermally ultrarelativistic limit ($\zeta_\infty \rightarrow 0$), whereas the difference is the most negligible factor in the nonrelativistic limit ($\zeta_\infty \rightarrow \infty$). Finally, the distribution function, $f(t, x^i, v^i)$ ($t > 0$), is at nonequilibrium state due to the initially curved spacetime. As an example of the nongravitational flow induced by gravitational-force-free particle motion in curved spacetime, we next analytically consider an initial nongravitational cluster inside the Schwarzschild radius of a thermally relativistic stuffed black hole.

A. Analytical consideration of an initial cluster inside a thermally relativistic stuffed black hole

A stuffed black hole [6] is a black hole whose inward spacetime of the Schwarzschild radius, R_s , is described using the FRW metric in the closed case and whose outward spacetime is described using the Schwarzschild metric. The particles inside R_s are uniformly distributed. When all the particles in a stuffed black hole are static (i.e., motionless and collisionless), the energy density of the stuffed black hole is defined using the mass energy density, nmc^2 . If the relativistic motion of particles inside R_s is non-negligible, however, the thermal energy density must be added to the mass energy density to define the energy density of the stuffed black hole. On the other hand, the thermal energy density is added to the mass energy density to also define the mass of the black hole.

Here, we consider a stuffed black hole that has relativistic thermal energy. For simplification, Hawking's radiation at R_s [7] is not considered here.

The initial gauge condition of a thermally relativistic stuffed black hole in isotropic coordinates [6] is

$$\begin{aligned} \alpha_0 &= 1, & \gamma_{ij,0} &= \delta_{ij} \phi_0^4, & \text{if } r < R_s, \\ \phi_0^4 &= 64 \left[1 + \left(\frac{2rc^2}{MG} \right)^2 \right]^{-2}, & & & \text{if } r > R_s, \\ \phi_0^4 &= \left(1 + \frac{MG}{2rc^2} \right)^{-4}, & r &= \sqrt{x_1^2 + x_2^2 + x_3^2}, \end{aligned} \quad (22)$$

where the subscript "0" indicates the initial state, M is the

mass of the black hole, G is the gravitational constant, δ_{ij} is Kronecker's delta function, and R_s is given by

$$R_s = \frac{MG}{2c^2} = \frac{1}{8} \sqrt{\frac{3c^4}{2\pi\tau_0 G}}, \quad \tau_0 = T^{00}|_{t=0}, \quad (23)$$

where τ is the energy density.

For simplicity, we use a spherically symmetric distribution function, $f(t, r, v^r) = f(t, r, v^r, \vartheta, \varphi)$, because $f(t, r, v^r, \vartheta, \varphi)$ is spherically symmetric owing to the spherical symmetry of the FRW metric and is uniform in the directions of ϑ and φ , where the Cartesian coordinates (x^1, x^2, x^3) are converted into spherical coordinates (r, ϑ, φ) via the relations $(x^1, x^2, x^3) = (r \sin \vartheta \cos \varphi, r \sin \vartheta \sin \varphi, r \cos \varphi)$ and $(v^1, v^2, v^3) = (v^r \sin \vartheta \cos \varphi, v^r \sin \vartheta \sin \varphi, v^r \cos \vartheta)$, in which $0 \leq \vartheta < \pi/2$ and $0 \leq \varphi < \pi$. Assuming that the number density is uniform (i.e., $n = n_\infty$), that the flow velocity is zero, and that the temperature is uniform (i.e., $\theta = \theta_\infty$), then from Eqs. (19) and (22), the initial equilibrium distribution function is $f^{(0)} = n_\infty / (4\pi m^2 c k \theta_\infty K_2) e^{-\zeta_\infty / \sqrt{1 - \phi_0^4(v^r)^2/c^2}}$, where $\zeta_\infty = mc^2 / (k \theta_\infty)$.

Figure 1 shows the initial state of the distribution function for three points, $i-1$, i , and $i+1$, along the radial axis r , where $r_{i-1}, r_i, r_{i+1} < R_s$. This figure reveals that the shape of the distribution function for each of these three points, $f^{(0)}(0, r^{i-1}, v^r)$, $f^{(0)}(0, r^i, v^r)$, and $f^{(0)}(0, r^{i+1}, v^r)$, depends on γ_{ij} given by Eq. (22) from Eq. (19). Here, we consider $f(\Delta t, r^i, v^r)$, where $\Delta t \ll 1$. For this case, the negative velocity tail of $f^{(0)}(0, r^{i+1}, v^r)$, which inflows into the negative tail of $f^{(0)}(\Delta t, r^i, v^r)$, is higher than that of $f^{(0)}(0, r^i, v^r)$, whereas the positive velocity tail of $f^{(0)}(0, r^{i-1}, v^r)$, which inflows into the positive tail of $f^{(0)}(\Delta t, r^i, v^r)$, is lower than that of $f^{(0)}(0, r^i, v^r)$. During Δt , the number of particles inflowing from r^{i+1} into r^i with the negative v^r is higher than that inflowing from r^{i-1} into r^i with the positive v^r . Consequently, $f(\Delta t, r^i, -|v^r|) > f(\Delta t, r^i, |v^r|)$ [16], thus leading to a negative flow velocity, which is equivalent to the cluster of a particle into the

origin, namely, the center of the black hole. Slicing parameters are determined to yield the constant local maximum speed c/ϕ_0^2 to avoid the numerical formation of tachyons, which is indicated by the inflow of particles in the shaded domain of $f^{(0)}(0, r^i, v^r)$ into r^{i-1} in Fig. 1. Such a set of slicing parameters in the Z4 formalism is described in Appendix B.

In the presence of particle collisions, such a cluster is confirmed numerically by simultaneously solving the non-gravitational general relativistic Anderson-Witting model and Einstein's equation based on the Z4 formalism. (The Z4 formalism is described in detail in Appendix B.)

The nongravitational general relativistic Anderson-Witting model indicated by $\psi^i = 0$ in Eq. (8) is written as follows [13]:

$$\frac{\partial f}{\partial t} + v^i \frac{\partial f}{\partial x^i} = \frac{U_L^\mu v_\mu}{c^2 \mathcal{T}} (f^{(0)} - f), \quad (24)$$

where $v_\mu = (\alpha^2 c, -v^j \gamma_{ij})$ and \mathcal{T} is the relaxation rate given by [17]

$$\mathcal{T} = \frac{1}{4n\pi\sigma v_s}, \quad (25)$$

$$v_s = \sqrt{\frac{\zeta^2 + 5G\zeta - G^2\zeta^2}{G(\zeta^2 + 5G\zeta - G^2\zeta^2 - 1)}} \frac{k\theta}{m}, \quad (26)$$

where $G \equiv K_3(\zeta)/K_2(\zeta)$, in which $K_3(\zeta)$ is the modified Bessel function of the third kind, and σ is the total cross section of the collision [13]. U_L^μ in Eq. (24) is the four-velocity of the flow defined by Landau-Lifshitz as [18]

$$U_L^\mu = U^\mu + \frac{q^\mu}{ne + p}, \quad (27)$$

where p is the static pressure defined as $p = nk\theta$.

The kinetic approach to the mesoscopic nonequilibrium induced by gravitational-force-free particle motion in curved spacetime is described in Appendix A.

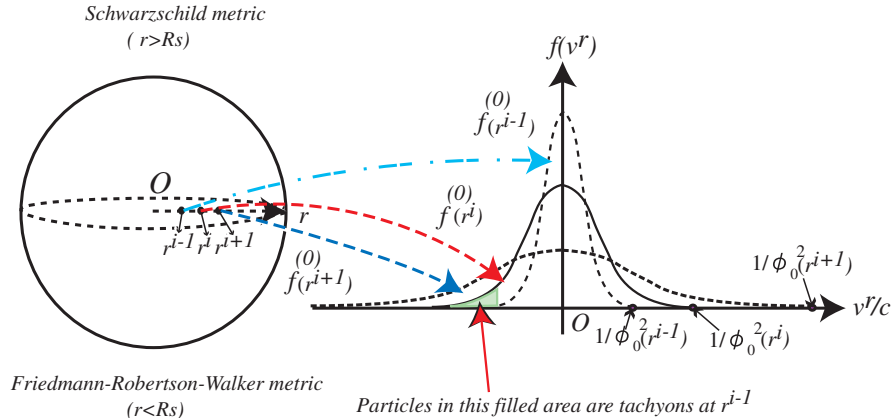


FIG. 1 (color online). Schematic of initial states of distribution functions of three points on radial axis.

B. Numerical analysis of initial nongravitational cluster inside a thermally relativistic stuffed black hole

For numerical analysis, we consider only the cubic domain $|x|, |y|, |z| \leq R_s/10$. The number density, velocity, temperature and gauge variables of the Z4 formalism at the boundary are fixed at their initial values. Once particles and gauge variables move from the calculated cubic domain to the outer boundary, they never return to the calculated cubic-domain. Namely, the nonreflecting boundary condition [19] is used. Consequently, the small jump in the variables at the boundary appears. The left-hand side of Eq. (23) is solved using the second-order total variation diminishing scheme [20]. The Z4 formalism for Einstein's equation is solved using the flux vector splitting scheme [21]. (The free parameters in the Z4 formalism are described in Appendix B.) For the numerical grid, we use the Cartesian grid, $(x, y, z, v^x, v^y, v^z) = (39, 39, 39, 48, 48, 48)$, which provides sufficiently accurate numerical results as discussed later in this section.

First, we nondimensionalize the macroscopic physical quantities and set $G/c^2 = 1/(n_\infty m L_\infty^2)$, where L_∞ is a representative length. Then, we set the normalized initial macroscopic quantities as $n/n_\infty = 1$, $\zeta_\infty = mc^2/(k\theta_\infty) = 45$ [22], and $u^i/c = 0$, and define the initial energy density τ in Eq. (B21) as $\tau_\infty/(n_\infty mc^2) = 1.032$, which yields $R_s/L_\infty = 0.085$ from Eq. (23), and $\mathcal{J}/t_\infty = 4\pi\sigma/L_\infty^2 = 10$ in Eq. (25). The initial conditions of the lapse α and intrinsic curvature γ_{ij} are given by Eq. (22). Einstein's equation is then modified using the results estimated using the nongravitational general relativistic Anderson-Witting model as indicated in Eqs. (B21)–(B23). Figure 2 shows the flow vectors at $t/t_\infty = 0.09$ and numerically confirms the cluster at the origin. Figure 3 shows the profile of the

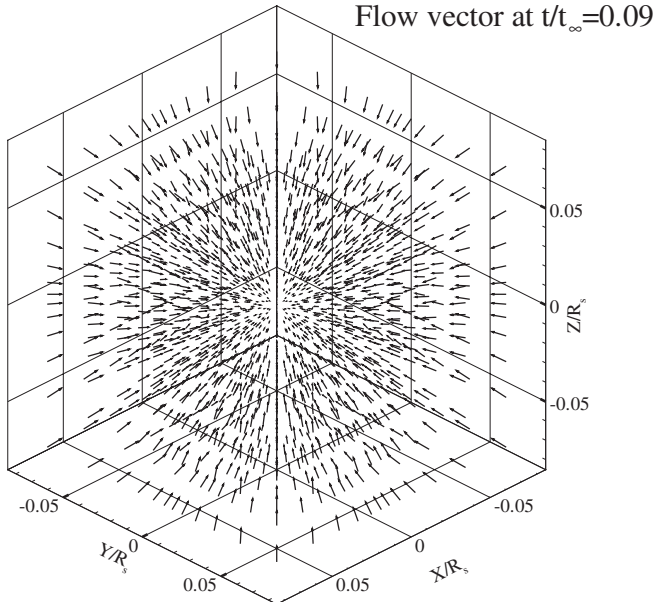


FIG. 2. Flow vectors in flowfield at $t/t_\infty = 0.09$.

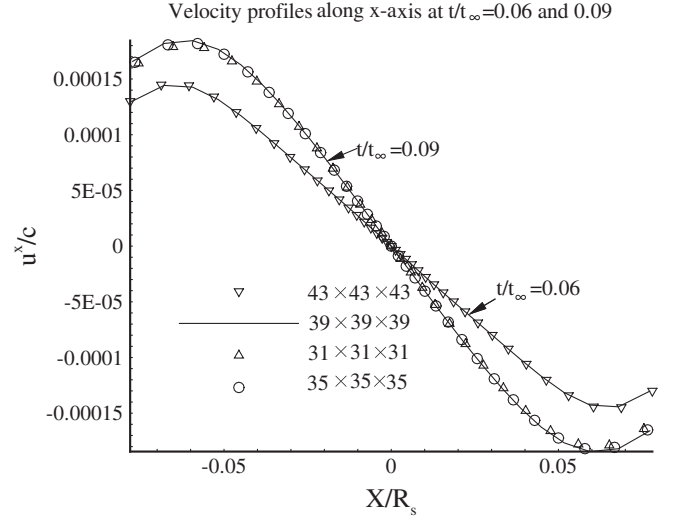


FIG. 3. Profiles of flow velocity u^x along x axis at $t/t_\infty = 0.06$ and 0.09 .

flow velocity of the x component, u^x/c , along the x axis at $t/t_\infty = 0.06$ and 0.09 . To confirm the numerical accuracy using the grid $(x, y, z) = (39, 39, 39)$, the profile obtained using the numerical grid $(x, y, z) = (43, 43, 43)$ at $t/t_\infty = 0.06$ and profiles obtained using grids $(x, y, z) = (31, 31, 31)$ and $(35, 35, 35)$ at $t/t_\infty = 0.09$ are compared with those obtained using the grid $(x, y, z) = (39, 39, 39)$ at $t/t_\infty = 0.06$ and 0.09 . Figure 3 shows this comparison, which confirms that the grid $(x, y, z) = (39, 39, 39)$ is sufficiently fine to achieve acceptable accuracy in the obtained numerical results. Figure 4 shows $f^{(0)}(v^x)/f(v^x) - 1$ at $x/R_s = \pm 0.052$ on the x axis at $t/t_\infty = 0.09$, where $f(v^x) \equiv \int_{\gamma^2} f dv^y dv^z$ and $f^{(0)}(v^x) \equiv \int_{\gamma^2} f^{(0)} dv^y dv^z$. As shown in Fig. 4, nonequilibrium at

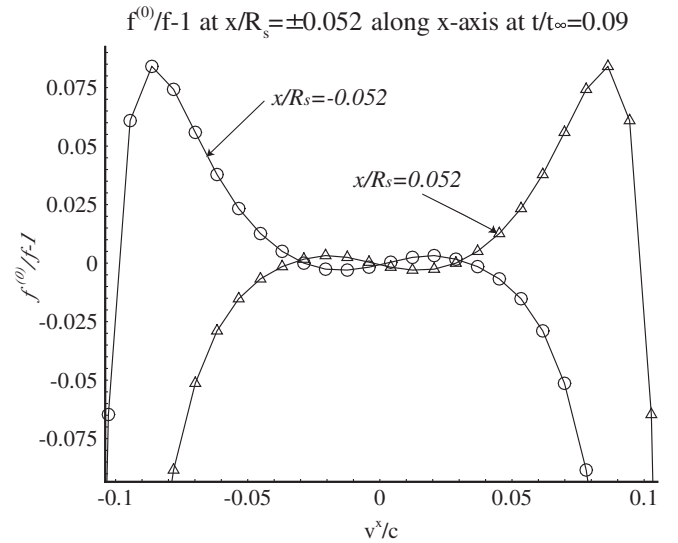


FIG. 4. Profiles of $f^{(0)}/f - 1$ at $x/R_s = \pm 0.052$ along x axis at $t/t_\infty = 0.09$.

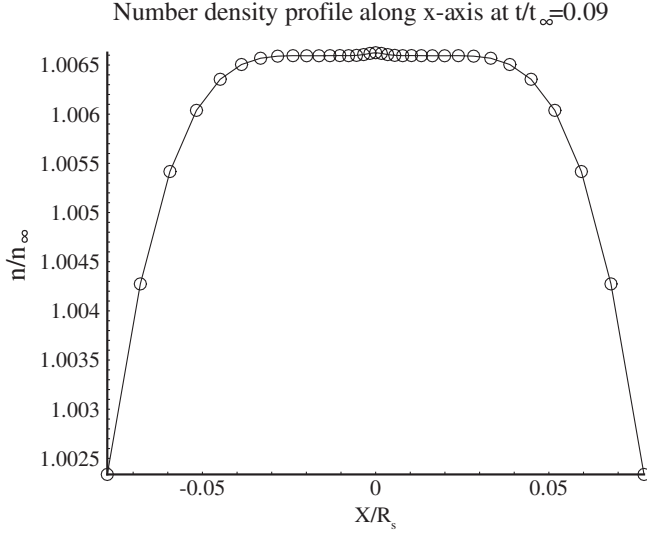


FIG. 5. Profile of number density (n) along x axis at $t/t_\infty = 0.09$.

both the negative and positive tails is significant for $x/R_s = \pm 0.052$. Figures 5–7 show the profiles of the number density (n), temperature (θ), heat flux in the x component (q^x), and dynamic pressure (ϖ), revealing that θ and ϖ exhibit peaks at the origin ($x/R_s = 0$) attributable to the compression. As shown in Fig. 6, q^x is proportional to the gradient of θ at $x/R_s \leq 0.052$, but is not proportional at $0.052 < |x/R_s|$ due to the relativistic effects. In addition to the gradient of temperature, other contributions to the heat flux include the contributions from the negative gradient of the pressure [24], from the gradient of the metric of the spacetime (described in Appendix A) and from terms above the Burnett order [25] are considered.

As shown in Fig. 7, ϖ is negative in all regimes, which is a trend opposite that of the positive ϖ introduced by the

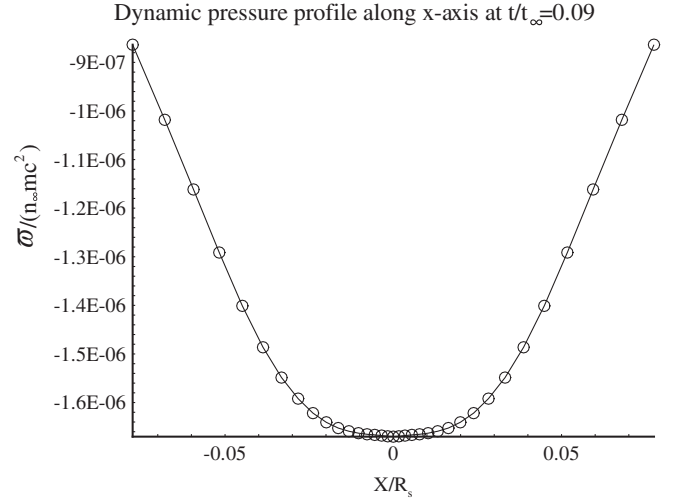


FIG. 7. Profile of dynamic pressure (ϖ) along x axis at $t/t_\infty = 0.09$.

14-moment Navier-Stokes-Fourier law for the contracting Universe [13]. Yano *et al.* [24] showed that the approximation of ϖ in the framework of the 14-moment Navier-Stokes-Fourier law must be confirmed by considering the contributions of the Burnett order terms to ϖ . In curved spacetime, the gradient of the metric of the spacetime (described in Appendix A) also affects ϖ .

Figure 8 shows profiles of the lapse α and local maximum speed v_m [$= v_{m,0}$ as defined in (B24)] along the x axis at $t/t_\infty = 0.09$. The profile of v_m is constant during the calculation ($0 \leq t/t_\infty \leq 0.09$), whereas α reaches its minimum at the origin and then increases with increasing $|x|$. The similar tendency of α to collapse has also been obtained [21] by solving only Einstein's equation without coupling to the kinetic equation, when the same slice condition is used.

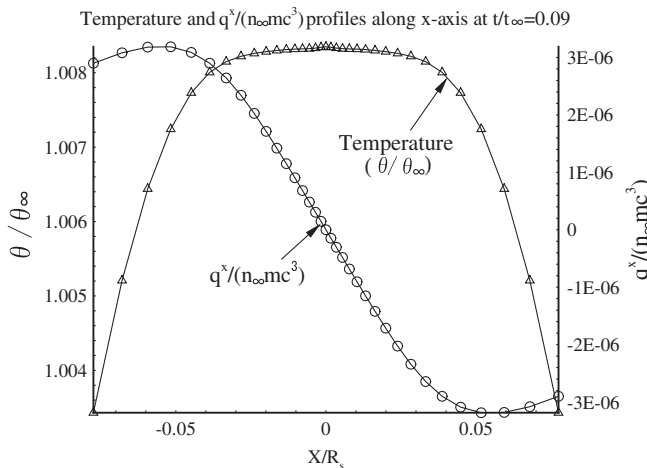


FIG. 6. Profiles of temperature (θ) (y_1 axis) and heat flux (q^x) (y_2 axis) along x axis at $t/t_\infty = 0.09$.

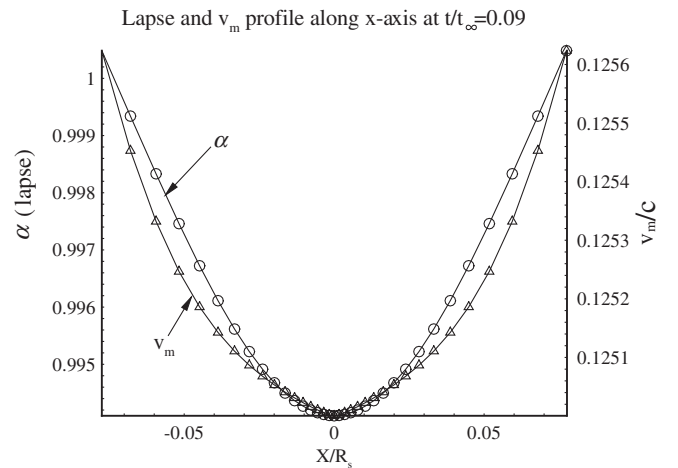


FIG. 8. Profiles of lapse (α) (y_1 axis) and local maximum speed v_m (y_2 axis) along x axis at $t/t_\infty = 0.09$.

IV. CONCLUDING REMARKS

The thermally relativistic flow induced by gravitational-force-free particle motion in curved spacetime is analyzed to investigate the specific property of thermally relativistic flows in the early Universe. As an object of analysis, the initial nongravitational cluster inside a thermally relativistic black hole is analyzed on the basis of the assumption that Hawking's radiation is negligible. When the equilibrium distribution function inside the Schwarzschild radius of a thermally relativistic stuffed black hole is known as initial data, the strict solution of the collisionless, non-gravitational general relativistic Boltzmann equation implies the incipient flow into the center of a black hole, a so-called initial cluster, inside the Schwarzschild radius. Such a cluster inside the Schwarzschild radius is confirmed in the presence of particle collisions by estimation using the nongravitational general relativistic Anderson-Witting model coupled to Einstein's equation, which is solved using the Z4 formalism. The obtained numerical results clearly confirm the presence of the initial cluster inside the Schwarzschild radius.

ACKNOWLEDGMENTS

We gratefully acknowledge C. Bona (Departament de Fisica, Universitat de les Illes Balears, Palma de Mallorca, Spain) for helpful comments on the numerics of the Z4 formalism. All calculations were executed using the supercomputer HITACHI SR11000 at the University of Tokyo through collaborative research with the Information Technology Center at the University of Tokyo.

APPENDIX A: EVALUATION OF NONGRAVITATIONAL NONEQUILIBRIUM CAUSED BY CURVED SPACETIME

The Chapman-Enskog expansion [26] is a useful tool for evaluating nonequilibrium caused by gradients in macroscopic quantities such as the number density, velocity and temperature. Because the form of the local equilibrium function depends on the metric of the curved spacetime (see Sec. III), the nonequilibrium caused by the gradient in this metric can be evaluated using conventional techniques, such as the Chapman-Enskog expansion.

Another form of the nongravitational general relativistic Anderson-Witting model is derived from Eq. (24) as follows:

$$p^\mu \frac{\partial f}{\partial x^\mu} = \frac{U_L^\mu p_\mu}{c^2 \mathcal{J}} (f^{(0)} - f). \quad (\text{A1})$$

As the first step in the Chapman-Enskog expansion, the equilibrium distribution function $f = f^{(0)}$ is substituted into the left-hand side of (A1) and $f = f^{(0)} + f^{(1)}$ is substituted into the right-hand side. To focus only on the nonequilibrium caused by the gradient of the metric, we assume that the number density, flow velocity, and tem-

perature are uniform, and thus Eq. (A1) can be rewritten as

$$\begin{aligned} p^\mu \frac{\partial g_{\nu\kappa}}{\partial x^\mu} \frac{\partial f^{(0)}}{\partial g_{\nu\kappa}} &= \frac{U_L^\mu p_\mu}{c^2 \mathcal{J}} \{f^{(0)} - (f^{(0)} + f^{(1)})\} \\ &= -\frac{U_L^\mu p_\mu}{c^2 \mathcal{J}} f^{(1)}. \end{aligned} \quad (\text{A2})$$

From the (3 + 1) ADM formalism with a zero shift and from the symmetric gauge condition as a result of Eq. (22) at $0 \leq t$, Eq. (A2) can be rewritten as

$$p^\mu \left(\frac{\partial \alpha^2}{\partial x^\mu} \frac{\partial f^{(0)}}{\partial \alpha^2} + \frac{\partial \phi^4}{\partial x^\mu} \frac{\partial f^{(0)}}{\partial \phi^4} \right) = -\frac{U_L^\mu p_\mu}{c^2 \mathcal{J}} f^{(1)}, \quad (\text{A3})$$

where $\gamma_{ii} = \phi^4$.

Then, using Eq. (19), $\partial f^{(0)}/\partial \alpha^2$ and $\partial f^{(0)}/\partial \phi^4$ in Eq. (A3) can be rewritten as

$$\frac{\partial f^{(0)}}{\partial \alpha^2} = f^{(0)} \zeta \left(\frac{\Gamma(u)^2 + \Gamma(v)^2}{2} \tilde{p}_\epsilon \tilde{U}^\epsilon - \Gamma(u)\Gamma(v) \right), \quad (\text{A4})$$

$$\frac{\partial f^{(0)}}{\partial \phi^4} = -f^{(0)} \zeta \frac{\tilde{p}_\epsilon \tilde{U}^\epsilon}{2} |\tilde{p}^i - \tilde{U}^i|^2, \quad (i = 1, 2, 3) \quad (\text{A5})$$

where $\tilde{p}^\epsilon = p^\epsilon/(mc)$ and $\tilde{U}^\epsilon = U^\epsilon/c$.

From Eqs. (A3)–(A5), $f^{(1)}$ is obtained as

$$\begin{aligned} f^{(1)} &= -\frac{c^2 \mathcal{J} \zeta}{U_L^\mu p_\mu} f^{(0)} \left\{ p^\mu (\alpha^2)_\mu \left(\frac{\Gamma(u)^2 + \Gamma(v)^2}{2} \tilde{p}_\epsilon \tilde{U}^\epsilon \right. \right. \\ &\quad \left. \left. - \Gamma(u)\Gamma(v) \right) - p^\mu (\phi^4)_\mu \frac{\tilde{p}_\epsilon \tilde{U}^\epsilon}{2} |\tilde{p}^i - \tilde{U}^i|^2 \right\}, \end{aligned} \quad (\text{A6})$$

where $(\alpha^2)_\mu \equiv \partial \alpha^2 / \partial x^\mu$ and $(\phi^4)_\mu \equiv \partial \phi^4 / \partial x^\mu$.

From Eq. (A6), the distribution function approximated using the Chapman-Enskog expansion is $f = f^{(0)} + f^{(1)}$. This procedure for $f^{(1)}$ from $f^{(0)}$ is repeated by substituting $\sum_{k=0}^{\mathcal{N}-1} f^{(k)}$ into the left-hand side of Eq. (A1) and $\sum_{i=0}^{\mathcal{N}} f^{(i)}$ into the right-hand side and assuming $\mathcal{N} \rightarrow \infty$.

Nonequilibrium terms, namely, $p^{(\mu\nu)}$, ϖ , and q^μ , in the Navier-Stokes-Fourier order ($\mathcal{N} = 1$) [5] are derived by first substituting $f = f^{(0)} + f^{(1)}$ into Eqs. (9) and (10) and then decomposing the obtained moments, N^μ and $T^{\mu\nu}$, using Eqs. (14)–(16). Owing to the terms $(\alpha^2)_\mu$ and $(\phi^4)_\mu$ in Eq. (A6), these three quantities ($p^{(\mu\nu)}$, ϖ , and q^μ) depend on the gradient of the metric.

Concrete formulations of $(\alpha^2)_\mu$ and $(\phi^4)_\mu$ in the Z4 formalism are readily introduced from Eqs. (B10), (B12), (B16), and (B17) in Appendix B.

APPENDIX B: Z4 FORMALISM

The first-order version of the Z4 formalism is written as [27]

$$\partial_t A_i + \partial_l [-\beta^l A_i + \delta^l_i (\alpha Q + \beta^m A_m)] = B_i^l A_l - B_l^l A_i, \quad \text{with the following definitions} \quad (\text{B1})$$

$$\begin{aligned} \partial_t B_k^i + \partial_l [-\beta_l B_k^i + \delta^l_k (\alpha Q_i + \beta^m B_m^i)] \\ = B_l^i B_k^l - B_l^l B_k^i, \end{aligned} \quad (\text{B2}) \quad D_i \equiv D_{ik}^k, \quad (\text{B8})$$

$$\begin{aligned} \partial_t D_{kij} + \partial_l [-\beta_l D_{kij} + \delta^l_k (\alpha Q_{ij} + \beta^m D_{mij})] \\ = B_k^l D_{lij} - B_l^l D_{kij}, \end{aligned} \quad (\text{B3}) \quad E_i \equiv D_{ki}^k. \quad (\text{B9})$$

$$\partial_t K_{ij} + \partial_k [-\beta^k K_{ij} + \alpha \lambda^k_{ij}] = S(K_{ij}), \quad (\text{B4})$$

In Eqs. (B1)–(B3), A_i, B_k^i and D_{kij} are defined as

$$\partial_t \Theta + \partial_k [-\beta^k \Theta + \alpha (D^k - E^k - Z^k)] = S(\Theta), \quad (\text{B5}) \quad A_i \equiv \partial_i \ln \alpha, \quad (\text{B10})$$

$$\partial_t Z_i + \partial_k [-\beta^k Z_i + \alpha \{-K^k_i + \delta^k_i (\text{tr} K - \Theta)\}] = S(Z_i), \quad (\text{B6})$$

$$B_k^i \equiv \partial_k \beta^i, \quad (\text{B11})$$

where λ^k_{ij} is defined with ordering parameter ξ as

$$\begin{aligned} \lambda^k_{ij} = D^k_{ij} - \frac{1}{2} (1 + \xi) (D_{ij}^k + D_{ji}^k) \\ + \frac{1}{2} \delta^k_i [A_j + D_j - (1 - \xi) E_j - 2Z_j] \\ + \frac{1}{2} \delta^k_j [A_i + D_i - (1 - \xi) E_i - 2Z_i], \end{aligned} \quad (\text{B7}) \quad D_{kij} \equiv \frac{1}{2} \partial_k \gamma_{ij}, \quad (\text{B12})$$

where β^i is the shift vector. Source terms in Eqs. (B4)–(B6) are [27]

$$\begin{aligned} S(K_{ij}) = & -K_{ij} B_k^k + K_{ik} B_j^k + K_{jk} B_i^k + \alpha \left\{ \frac{1}{2} (1 + \xi) \left[-A_k \Gamma_{ij}^k + \frac{1}{2} (A_i D_j + A_j D_i) \right] \right. \\ & + \frac{1}{2} (1 - \xi) \left[A_k D^k_{ij} - \frac{1}{2} \{ A_j (2E_i - D_i) + A_i (2E_j - D_j) \} + 2(D_{ir}^m D^r_{mj} + D_{jr}^m D^r_{mi}) - 2E_k (D_{ij}^k + D_{ji}^k) \right] \\ & + (D_k + A_k - 2Z_k) \Gamma_{ij}^k - \Gamma_{mj}^k \Gamma_{ki}^m - (A_i Z_j + A_j Z_i) - 2K^k_i K_{kj} + (\text{tr} K - 2\Theta) K_{ij} \Big\} \\ & - 8\pi\alpha \left[S_{ij} - \frac{1}{2} \gamma_{ij} (-\tau + S^k_k) \right], \end{aligned} \quad (\text{B13})$$

$$\begin{aligned} S(Z_i) = & -Z_i B_k^k + Z_k B_i^k + \alpha [A_i (\text{tr} K - 2\Theta) - A_k K^k_i \\ & - K^k_r \Gamma_{ki}^r + K^k_i (D_k - 2Z_k)] - 8\pi\alpha S_i, \end{aligned} \quad (\text{B14})$$

$$\begin{aligned} S(\Theta) = & -\Theta B_k^k + \frac{\alpha}{2} [2A_k (D^k - E^k - 2Z^k) + D_k^{rs} \\ & + \Gamma_{rs}^k - D^k (D_k - 2Z_k) - K^k_r K^r_k \\ & + \text{tr} K (\text{tr} K - 2\Theta)] - 8\pi\alpha \tau. \end{aligned} \quad (\text{B15})$$

In Eq. (B12), the intrinsic curvature γ_{ij} is then given by

$$\partial_t \gamma_{ij} + \partial_l [-\beta^l \gamma_{ij}] = -2\alpha K_{ij}, \quad (\text{B16})$$

where K_{ij} is the extrinsic curvature.

In Eq. (B1), Q is the rate of temporal variation of α as

$$\partial_t \alpha = -\alpha^2 Q, \quad (\text{B17})$$

and is expressed in harmonic coordinates as [27]

$$Q = -a \frac{\beta^k}{\alpha} \partial_k \ln \alpha + F(\alpha) (\text{tr} K - \eta \Theta). \quad (\text{B18})$$

In Eq. (B18), $F = 0$ corresponds to geodesic slicing, $F = 1$ corresponds to harmonic slicing, and $F = 2/\alpha$ corresponds to “1 + log” slicing. In Eq. (B2), Q^i is the rate of the temporal variation of β^i as

$$\partial_t \beta^i = -\alpha Q^i, \quad (\text{B19})$$

and Q^i is expressed in harmonic coordinates as [27]

$$Q^i = -\frac{\beta^k}{\alpha} \partial_k \beta^i - \alpha \gamma^{ki} (\partial^j \gamma_{jk} - \partial_k \ln \sqrt{\gamma} - \partial_k \ln \alpha). \quad (\text{B20})$$

In our numerical analysis, the shift β^i , the free parameter ξ in Eq. (B7), and η in Eq. (B18) are all set to zero, and the

initial values of A_i , B_k^i , K_{ij} , Θ , and Z_i are also all set to zero.

When $\beta^i = 0$, the energy density τ , momentum density S_i , and stress tensor S_{ij} are given by [8]

$$\tau \equiv \alpha^2 T^{00}, \quad (\text{B21})$$

$$S_i \equiv \alpha T_i^0, \quad (\text{B22})$$

$$S_{ij} \equiv T_{ij}. \quad (\text{B23})$$

The propagation of gauge variables via the Z4 formalism occurs at its characteristic speed [21] regardless of the hydrodynamic propagations of particles as indicated by the left-hand side of Eq. (24). Consequently, the constraint $0 < \alpha^2 - \hat{v}^2$ in Eq. (4) is violated, if the gauge evolves freely from such a constraint. Here, we describe a set of slicing parameters that does not violate the constraint $0 < \alpha^2 - \hat{v}^2$ reasonably.

The initial local maximum speed $v_{m,0}$ is defined from Eqs. (4) and (22) as

$$v_{m,0} \equiv \frac{\alpha_0 c}{\phi_0^2}. \quad (\text{B24})$$

Assuming that $v_{m,0}$ during the calculation is equal to its initial value, F in Eq. (B15) is fixed at $F = 1/3$, which gives the following relation from Eqs. (B16)–(B18):

$$\frac{\alpha}{\alpha_0} = \left(\frac{\gamma}{\gamma_0} \right)^{(1/6)}, \quad (\text{B25})$$

where the subscript “0” indicates an initial state and $\gamma \equiv \det(\gamma_{ij})$. In our analysis, $\gamma_{xx} = \gamma_{yy} = \gamma_{zz} = \phi^4$, and the other elements of γ_{ij} are zero because the spherically symmetric field is conserved during the calculation. Consequently, from Eq. (B25), $\gamma = \gamma_{xx}\gamma_{yy}\gamma_{zz} = \phi^{12}$ yields the relation $v_m \equiv \alpha c / \phi^2 = v_{m,0}$. The assumption of constant v_m is based on the conjecture that the number of particles that inflow from other spatial points at which the particles have velocity higher than v_m , is negligible. Particles whose velocity exceeds v_m , such as tachyons, are excluded. Such particles are present inside the shaded domain shown in Fig. 1.

-
- [1] H. Sato, Prog. Theor. Phys. **63**, 6, 1971 (1980).
 - [2] A. Membrilla and M. Bellini, Phys. Lett. B **635**, 5, 243 (2006).
 - [3] R.W. Wald, *General Relativity* (The University of Chicago Press, Chicago, 1984).
 - [4] J.I. Kapusta, Phys. Rev. Lett. **86**, 1670 (2001).
 - [5] C. Cercignani and G.M. Kremer, *The Relativistic Boltzmann Equation: Theory and Applications*, Progress in Math. Phys. (Springer-Verlag, Berlin, 2002), Vol. 22.
 - [6] A. Arbona, C. Bona, J. Carot, L. Mas, J. Masso, and J. Stela, Phys. Rev. D **57**, 2397 (1998).
 - [7] S.W. Hawking, Phys. Rev. D **72**, 084013 (2005).
 - [8] C. Bona and C. Palenzuela-Luque, *Elements of Numerical Relativity; From Einstein's Equations to Black Hole Simulations*, Lecture Notes in Phys. (Springer, New York, 2005).
 - [9] D. Alic, C. Bona, and C. Bona-Casas, Phys. Rev. D **79**, 044026 (2009).
 - [10] J. Yokoyama, Phys. Rev. D **58**, 107502 (1998).
 - [11] G.L. Alberghi, R. Casadio, and A. Tronconi, J. Phys. G **34**, 767 (2007).
 - [12] S.W. Hawking, Commun. Math. Phys. **43**, 199 (1975).
 - [13] G.M. Kremer and F.P. Devecchi, Phys. Rev. D **65**, 083515 (2002).
 - [14] R. Arnowit, S. Deser, and C.W. Misner, in *Gravitation: An Introduction to Current Research*, edited by L. Witten (Wiley, New York, 1962).
 - [15] C. Eckart, Phys. Rev. **58**, 919 (1940).
 - [16] This relation is proven by $f(\Delta t, r, v^r) = f^{(0)}(0, r - v^r \Delta t, v^r) \leq f(\Delta t, r, -v^r) = f^{(0)}(0, r + v^r \Delta t, -v^r)$ for $0 \leq v^r$.
 - [17] v_s defined by Eq. (26) is originally introduced for the special relativistic Anderson-Witting model. However, we apply v_s to the nongravitational general relativistic Anderson-Witting model, because the introduction of v_s is difficult.
 - [18] L.D. Landau and E.M. Lifshitz, *Fluid Mechanics* (Pergamon Press, Oxford, 1987), 2nd. ed..
 - [19] D. Givoli, J. Comp. Physiol. **94**, 1, 1 (1991).
 - [20] H.C. Yee, *A Class of High-Resolution Explicit and Implicit Shock-Capturing Methods: Lecture Series Vol. 4*, (von Karman Institute for Fluid Dynamics, Rhode-St-Genese, Belgium, 1989).
 - [21] R. Yano, K. Suzuki, and H. Kuroda, arXiv:0810.0627v1.
 - [22] $\zeta = mc^2/(k\theta) = 45$ gives $\theta \sim 4.3 \times 10^8$ [K], when $m = 1.5$ [MeV], which is similar to the mass of the up quark [23]. The total static mass, M_{stat} , of the black hole determined from Hawking's radiation, $\theta = \hbar^3 c^3 / (8\pi M_{\text{stat}} k)$, is $M_{\text{stat}} \sim 8.2 \times 10^{12}$ [kg]. Consequently, the total number of particles is $M/m = 3.0 \times 10^{42}$ and the Schwarzschild radius, 1.8×10^{-15} [m], is much longer than the Planck length, 1.6×10^{-35} [m], and similar to the radius of a hydrogen nucleus, 10^{-15} [m]. If particles are uniformly distributed inside the Schwarzschild radius, the length appropriated by one particle is approximately 2×10^{-29} [m], which is much smaller than the radius of an electron 10^{-18} [m].
 - [23] K. Yagi, T. Hatsuda, and Y. Miyake, *Quark-Gluon Plasma: From Big Bang to Little Bang* (Cambridge University Press, New York, 2005).
 - [24] R. Yano, K. Suzuki, and H. Kuroda, Physica A (Amsterdam) **381**, 8 (2007).

- [25] L.L. Samojeden and G.M. Kremer, *Physica A* (Amsterdam) **307**, 354 (2002).
- [26] S. Chapman and T.G. Cowling, *Mathematical Theory of Non-Uniform Gases* (Cambridge University Press, Teddington, England, 1939).
- [27] C. Bona, L. Lehner, and C. Palenzuela-Luque, *Phys. Rev. D* **72**, 104009 (2005).